

Pawel MACIOLKA<sup>1\*</sup>

## **EXPERIMENTAL INVESTIGATION OF FLAT SURFACES IN CONTACT**

This paper presents a method of measuring deformations in the contact between flat surfaces and a way of estimating the shares of elastic and plastic deformations in the total contact deformations. Experiments showed that the share of plastic deformations in the total contact deformations varied depending on the strength parameters of the specimens and the roughness parameters of the contacting surfaces, amounting to a few per cent and to 37% for respectively steel specimens and specimens made of aluminium alloy AW5754. A strategy for estimating all the deformation components for the tested specimen types and the kinds of machining is presented.

### **1. INTRODUCTION**

The experiments presented in this paper are the continuation of the research aimed at developing a simple method of determining the characteristics of the contact between two rough surfaces under load. The experiments were carried out on a specially designed measuring stand ensuring – thanks to the unique openwork structure of the loading assembly – high precision of the measurement of the deformations occurring in contacts loaded with a normal force [1]. The experimental results will be used to model and determine the theoretical characteristics of the contact. Thanks to the models it will be possible to control the fixing force which affects workpiece machining accuracy, which in turn depends on the contact deformations not only during machining, but also during positioning and fixing workpieces in production jigs. An exemplary characteristic of the contact is shown in Fig. 1.

After fixing the workpiece it is often essential to control the fixing force, particularly when it is to be kept at a precisely specified level, e.g. to ensure its optimal value. The force may vary even when the position of the actuator fixing the workpiece is constant. An analysis of a hypothetical case of an unexpected increase in the loading force in the place of fixing (the 2nd loading), due to the effect of the cutting process on the fixture, shows that even though the cutting ceased (the 2nd unloading), the fixing force decreased.

---

<sup>1</sup> Wroclaw University of Technology, Department of Machine Tools and Mechanical Technologies, Wroclaw, Poland

\* E-mail: pawel.maciolka@pwr.edu.pl

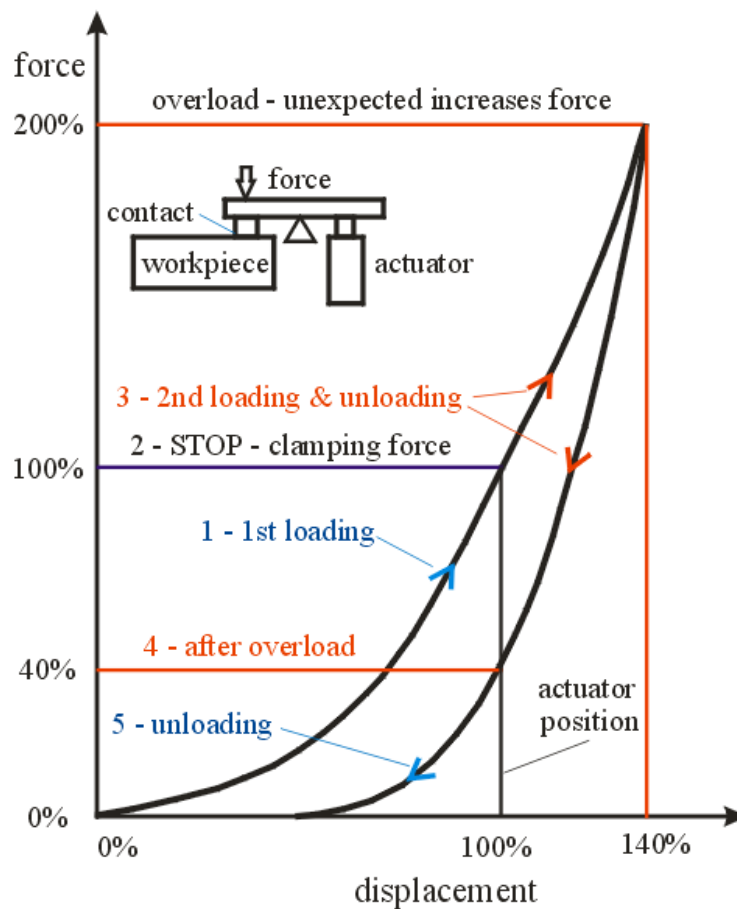


Fig. 1. Exemplary characteristic of contact between rough surfaces of workpiece and fixture

It emerges from Fig. 1 that the instantaneous overloading of the contact with a force twice greater than the fixing force causes a drop in the fixing force to 40% of its initial value. This behaviour is due to the fact that the loading curve and the unloading curve do not coincide and that the position of the actuator remains unchanged.

## 2. MEASURING STAND

Contact characteristics were investigated on the measuring stand shown in Fig. 2. More information about the design and properties of this stand can be found in the previous work by the author [1]. The stand structure makes it possible to quickly fix specimens in plane XY in any place on the table and load them solely with a force normal to the specimen surface. For this purpose specimens with vacuum fixing and a special movable member cut in the test stand, ensuring displacements solely along the direction of loading, had to be designed. Load-bearing strips, uniquely connecting the movable member with the stand in plane XY, were obtained by cutting channels in the stand frame. The strips can elastically bend only in direction Z.

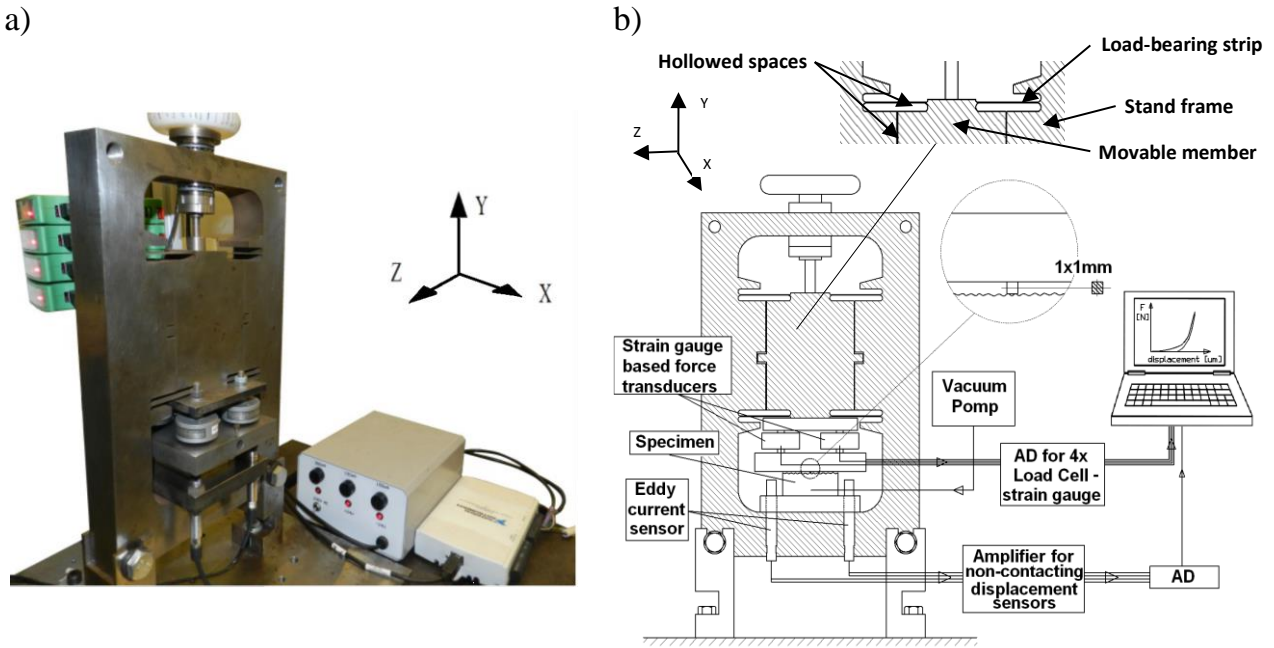


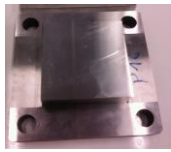

Fig. 2. Measuring stand: a) view, b) schematic

### 3. TYPES OF SPECIMENS

Steel and aluminium specimens, made in two versions (Table 1): as specimens vacuumed fixed to the stand table (specimens A) and specimens together with tables fixed with screws to the stand (monolithic specimens B).

Table 1. Types and characteristics ( $S_a$  - average roughness,  $S_z$  - maximum height of surface) of specimens

Name	View	Material	Machining	Fixing	$S_a$ [ $\mu\text{m}$ ]	$S_z$ [ $\mu\text{m}$ ]
Specimen A		steel (NC10)	grinding	by vacuum to table	0.18	2.57
		aluminium alloy (AW5754)	milling	by vacuum to table	2.24	13.34
			sandblasting		2.60	40.01

Specimen B		steel (45)	grinding	by screw to frame	0.24	4.40
		aluminium alloy (AW5754)	milling	by screw to frame	2.75	17.40

The preparation and use of specimens B is more time-consuming since it necessitates the disassembly and reassembly of four displacement sensors due to the fact that roughness measurements are carried out almost after each load cycle.

Specimens A were prepared for vacuum fixing. They have special channels and seals (Fig. 3). When connected to a working vacuum system such a specimen owing to the produced vacuum is pressed down to the table equipped with four displacement sensors. In this case, the mounting and dismounting of the specimen do not necessitate the disassembly/reassembly of the displacement sensors. Since the sensors are attached not to the specimen, but to the table the sensors measuring the displacements of the punch also measure the displacements resulting from the deformations taking place in the table/specimen contact. Thus, besides the investigated punch/specimen contact, an additional contact with unknown stiffness arises. The latter contact can be taken into account in the investigations or omitted. Monolithic specimens B were prepared in order to find out how important this component is and how it affects the accuracy of the measurement of the punch/specimen contact characteristic.

Specimen type B was obtained by making the specimen and the table out of one piece of metal, whereby the additional contact, which posed a significant problem in the case of specimens A, was eliminated (Fig. 4).

The specimens were made of alloy AW5754 and steel 45 and NC10. The specimen surfaces being in contact with the punch were mechanically machined by grinding, milling and sandblasting.

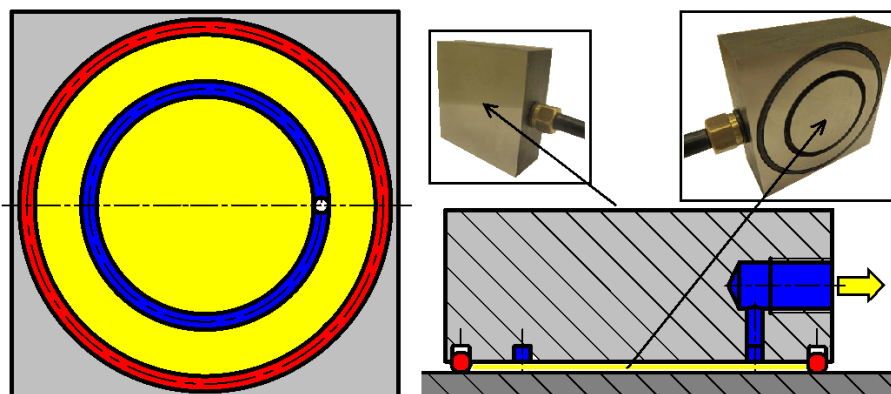


Fig. 3. Structure of specimen A with vacuum fixing system [1]

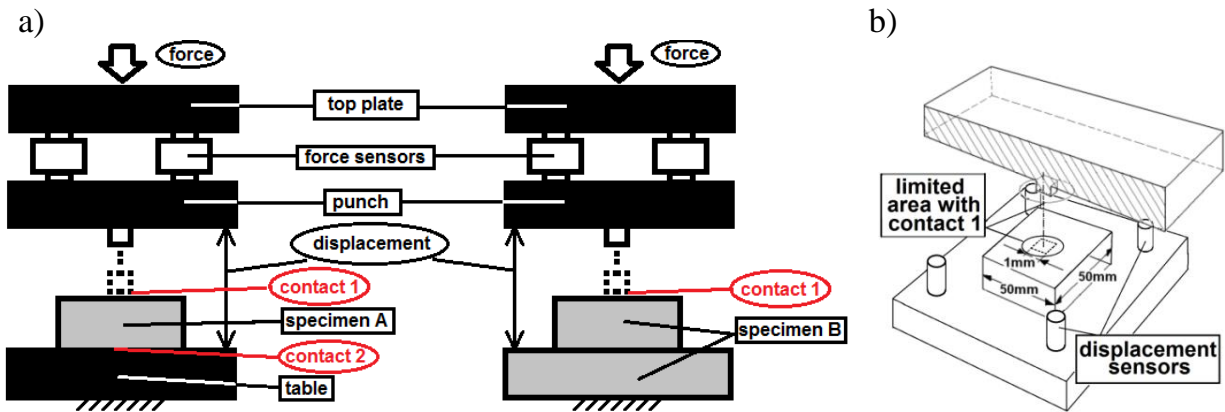


Fig. 4. Specimen/punch system: a) contact loading, b) contact between punch and specimen B

A Tallysurf CCI Lite profilometer was used to measure the surface roughness. Measurement techniques of the surface geometric structure based on white light have been widely applied on supervising of cutting process [7], wear process [8] and improving of tribological properties of sliding [2]. Selected surface roughness parameters:  $S_a$  – average roughness and  $S_z$  – maximum height of surface ( $9 \text{ mm}^2$ ) are shown in Table 1.

#### 4. FE MODEL OF SPECIMEN-PUNCH SYSTEM DEFORMATIONS

The specimen-punch system characteristic obtained from Finite Element (FE) modelling was used to determine the characteristics describing solely the nonlinear elastic deformations taking place in the contact. The following were used in the model with specimen A and B (Fig. 5):

- hexagonal solid finite elements with a linear shape function,
- Young's modulus  $E=220\text{GPa}$  (steel),  $75\text{GPa}$  (alloy AW5754),
- Poisson ratio  $\nu=0.3$ ,
- type of contact: hard in the normal direction and frictionless in the tangential direction.

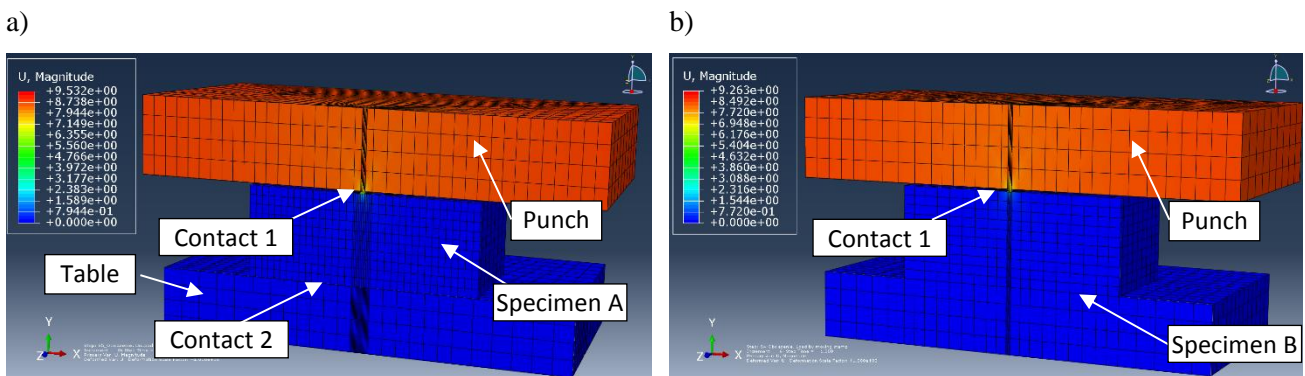


Fig. 5. FE model calculation of displacements in specimen-punch system under load of 400N:  
a) steel specimen of type A, b) steel specimen of type B

This above was tantamount to the assumption of high stiffness of the contacts and linear elasticity of the system. The contact places were discretized using the surface to surface method. In the place where the table was fixed to the frame, the former was deprived of the possibility of moving in directions X, Y and Z. The loading and unloading of the specimen was effected by moving the punch only along axis Y. The punch would be moved by a set value corresponding to the force with which the specimen was loaded during the experiment. Figure 5 shows an example of calculations of punch displacements relative to the surface of a steel specimen of type A and B.

## 5. ASSESSMENT OF ADDITIONAL CONTACT SHARE

In the experiments the additional contact occurred only in the case of vacuumed fixed specimen type A. The results obtained for milled specimen A made of the aluminium alloy were compared (Fig. 6) with the appropriate measurement for specimen B in the case of which only one specimen/punch contact occurs.

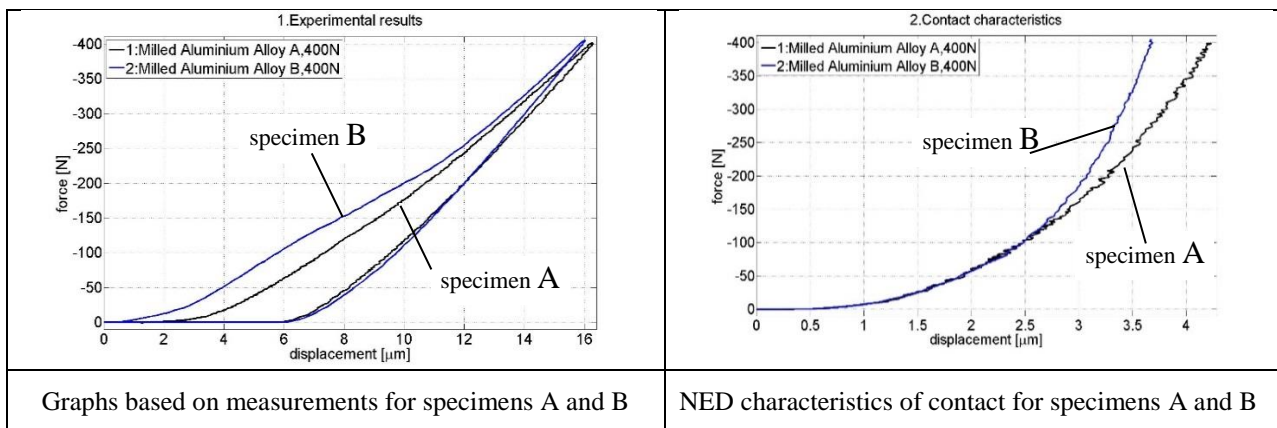


Fig. 6. Contact characteristics for milled aluminium alloy specimens A and B

The maximum displacements measured in both cases when the specimen was loaded with a force of 400 N by the punch are similar (16.0 and 16.3  $\mu\text{m}$ ). The only reason why one could expect larger displacements for specimen A can be the nonlinear elastic deformations and plastic deformations in the additional contact, which should add to the deformations in the specimen/punch contact. It appears from the experimental nonlinearly elastic characteristics that no plastic deformations occurred in the additional contact between specimen A and the table since the difference of 0.5  $\mu\text{m}$  indicated by the measurements occurred wholly in the nonlinear elastic deformations. Considering the absence of plastic deformations and the very small differences between the nonlinearly elastic deformations, the effect of the additional contact whose nominal surface area is 2500 times larger than that of the specimen/punch contact can be regarded as insignificant.

Unique procedures for extracting information from the measurement curves had to be worked out to determine the nonlinearly elastic characteristics of the contact and to estimate the percentage of plastic deformations.

## 6. ANALYSIS-AIDING PROCEDURES

The aim of the developed analysis-aiding procedures was to objectively estimate the share of each of the three deformation components (LED, PD, NED) in the specimen-punch system or the table-specimen-punch system, causing the displacements measured during the experiments.

The slope of the displacement= $f$ (force) characteristic (Fig. 7a) measured on the test stand is determined by:

- linear elastic deformations (LED),
- plastic deformations (PD),
- nonlinear elastic deformations (NED).

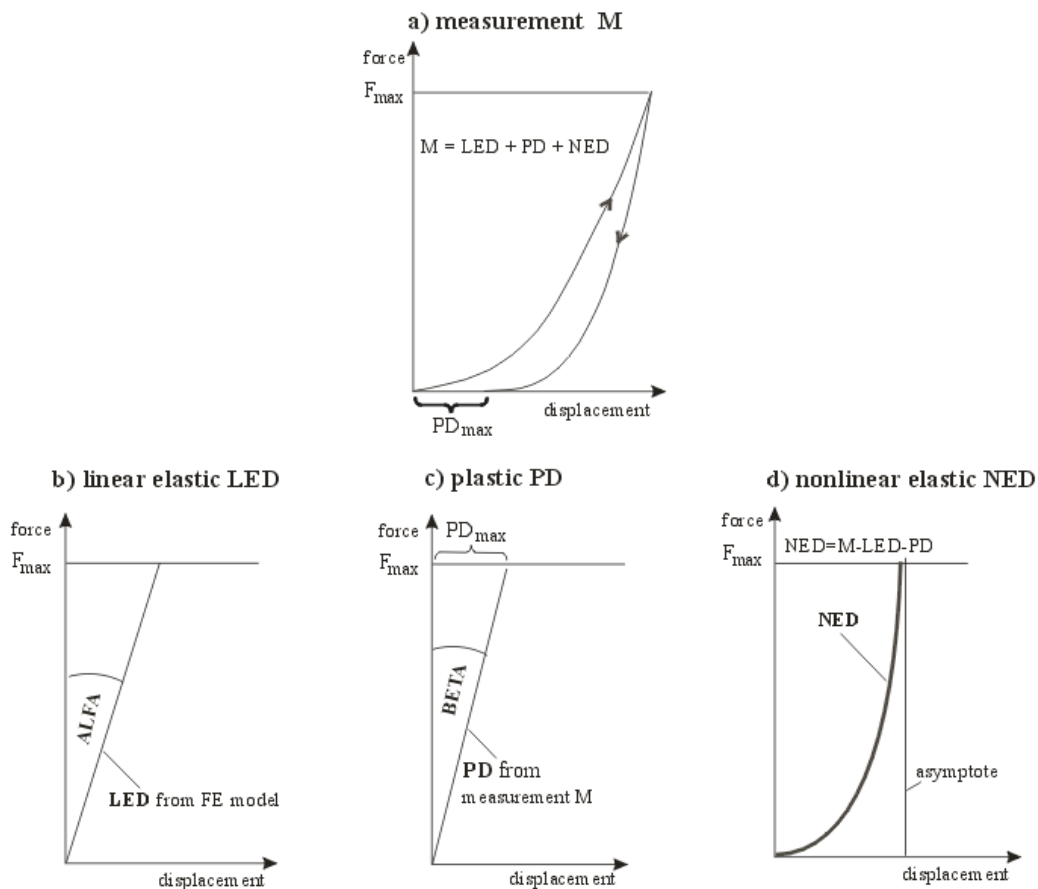


Fig. 7. Procedure for predicting elastic deformations in contact: a) measurement cycle on test stand, b) linear elastic deformations, c) plastic deformations, d) characteristic of nonlinear elastic deformations in contact

Linear elastic deformations (LED) (Fig. 7b) can be determined through modelling. Knowing LED one can estimate the share of plastic deformations (PD), if such still occurred (Fig. 7c), in any measurement. Prior to this, from first-cycle measurement M one must determine the maximum value of plastic deformations  $PD_{max}$  which will remain after contact unloading (Fig. 7a). As a result, it becomes possible to determine the nonlinear elastic deformations (NED) in the contact by subtracting the linearly elastic deformations and the plastic deformations (LED+PD) from the measured characteristic M (Fig. 7d).

In works dealing with contact problems one can find an assumption that plastic deformation increments in a contact are approximately directly proportional to the increments in the loading force [3],[4],[5]. Another simplification adopted for the needs of the proposed procedure is the assumption that the first plastic deformations occur already at the zero force value. In reality, a certain relatively small force which will produce stresses higher than the plastic limit in the asperities is always needed. Also the geometry of the specimen surface changes as a result of the plastic deformations, which is another reason why the decay of elastic deformations in the unloading phase proceeds differently than their growth during loading [3]. The above procedures enable one to estimate the share of each of the components (LED, PD and NED) in the total values registered during any measuring cycle.

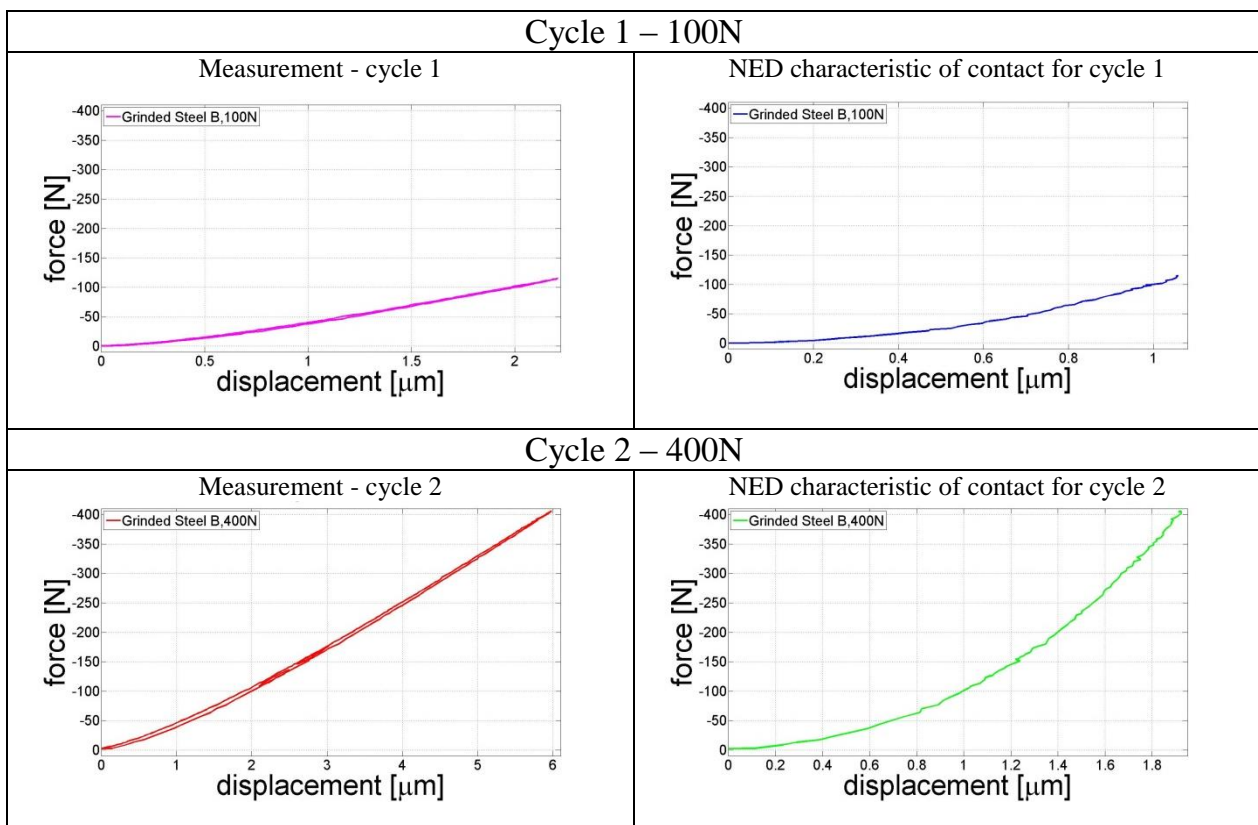


Fig. 8. Analysis of measurement cycle carried out for ground steel specimen B: a) first loading (cycle 1), b) second loading (cycle 2)



Figure 8 shows the measurement results obtained in the first loading of the specimen up to a force of 100 N (cycle 1) and its reloading with the maximum force of 400 N (cycle 2). The ground steel sample B was loaded with a polished steel punch  $1 \text{ mm}^2$  in cross section. Plastic deformations still occurred in the two cycles. In cycle 1 this was due to the fact that it was the first loading of the specimen while in cycle 2 the reason was the exceedance of the maximum loading force of the previous cycle. According to the proposed procedure, nonlinearly elastic characteristics of the contact were determined for the two measurements. As expected, the characteristics are identical and attempts at reading the values of nonlinear elastic deformations (NED) from each of the characteristics lead to similar results. For example, the deformation value for 100 N, read from the characteristic determined by decomposing cycle 1 amounts to about  $1 \mu\text{m}$  and the one read from the characteristic determined by decomposing cycle 2 amounts also to  $1 \mu\text{m}$ .

Following the procedures the characteristics of nonlinear elastic deformations (NED) and plastic deformations (PD) in the investigated contacts, shown in Fig. 9, were obtained. However, one should bear in mind that in the case of specimens A these are the combined characteristics of the investigated contact and the additional contact (the influence of the latter is negligible).

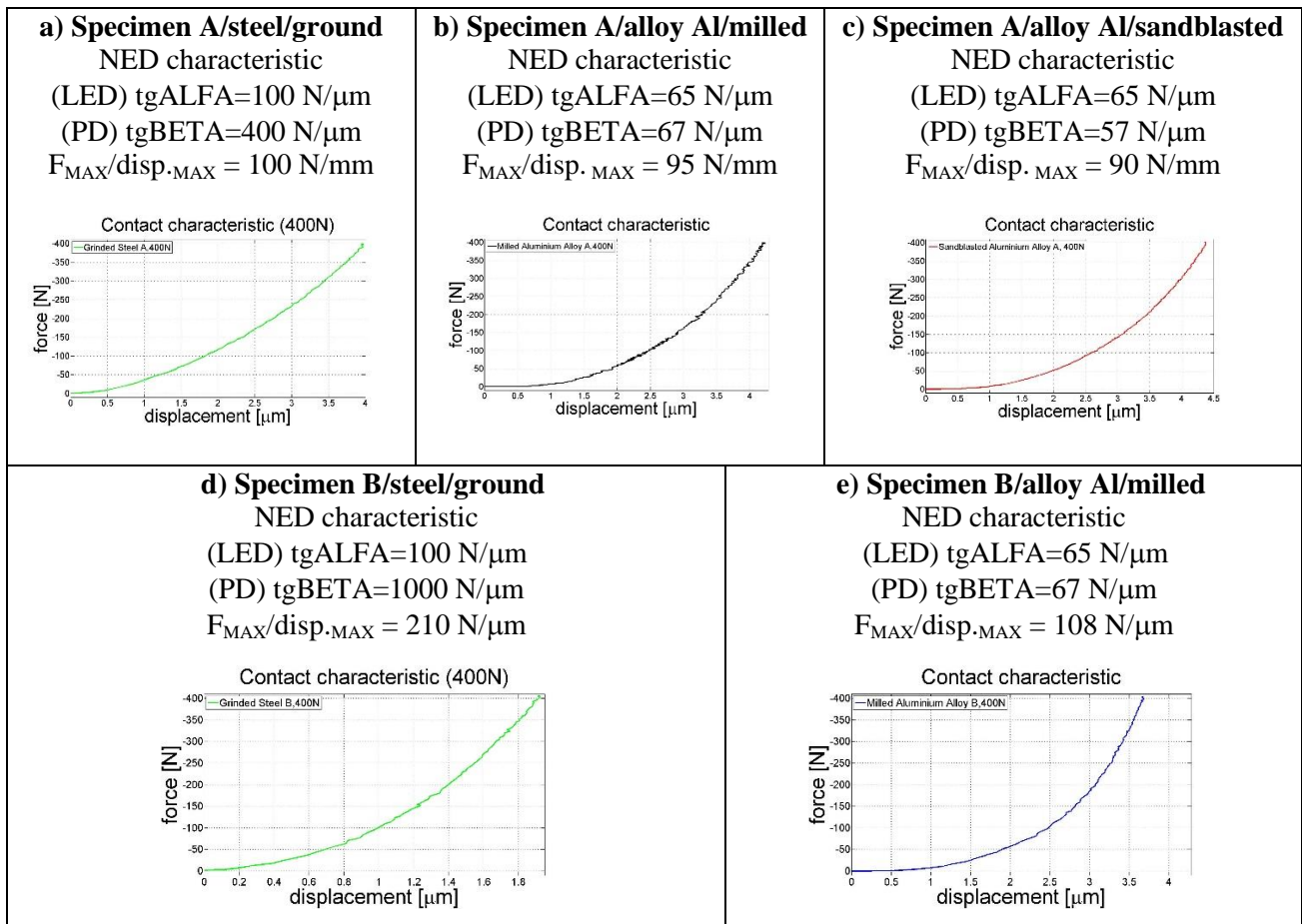


Fig. 9. Characteristics of nonlinearly elastic deformations (NED) and angular coefficients of LED and PD of tested contacts (polished steel punch  $1 \text{ mm}^2$  in cross section)

### 7. TESTS OF ALUMINIUM SPECIMENS

Large plastic deformations are characteristic of the tests of the aluminium specimens. This can be observed in the form of a track of the punch on the specimen after the first loading. From the surface topography, with visibly deformed microridges and probably intact valleys, shown in Fig. 10 one can read the value of the plastic deformations, which under the load of 400 N amounted to about 6  $\mu\text{m}$  for the milled specimen. In the case of the sandblasted specimen the deformation amounted 7 $\mu\text{m}$ .

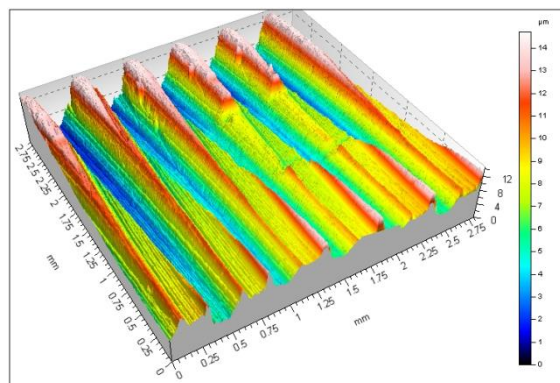


Fig. 10. Surface topography after specimen AW5754 was loaded with force of 400 N

The share of plastic deformations in the total measured displacements is much bigger than in the case of the steel specimens. The shares which make up the measured displacement value are shown in Table 2.

Table 2. Shares of component deformations in measured displacement for load of 400N

FORECAST for 400N: (Unloading from:100N&400N)	Specimen made of Al alloy						Steel specimen			
	A/AL./SB		A/AL./M		B/AL./M		A/St/G		B/St/G	
Deformation	$\mu\text{m}$	%	$\mu\text{m}$	%	$\mu\text{m}$	%	$\mu\text{m}$	%	$\mu\text{m}$	%
- nonlinear NED:	4.4	26	4.3	27	3.7	24	4.0	44	1.9	30
- plastic PD:	6.2	37	5.5	35	5.5	36	1.0	12	0.4	6
- linearly elastic LED:	6.1	37	6.1	38	6.1	40	4.0	44	4.0	63
Deformation M = NED+PD+LED	16.7	100	15.9	100	15.3	100	9.0	100	6.3	100
M - measured for 400N (from roughness profiles):	16.5	100	15.7	100	15.2	100	8.5	100	6.0	100

According to the Table 2 in the case of the aluminium specimens the plastic deformations amount to 35–37%. the nonlinear elastic deformations to 24–27% and the linearly elastic deformations to 37–40% of the total deformations. For the steel specimens the share of plastic deformations is three times smaller (6–11%). This means that the kind

of machining has a less significant bearing on contact stiffness. This is confirmed by the test results for the two kinds of machining applied to aluminium specimens A (Fig. 11).

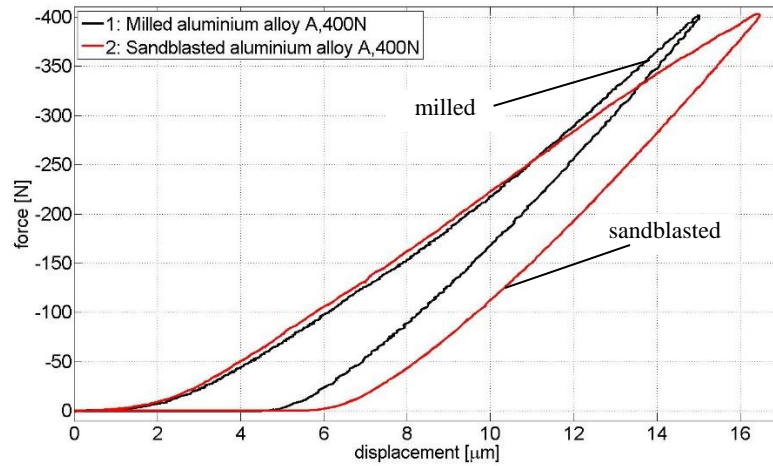


Fig. 11. Cycle of loading respectively milled and sandblasted aluminium specimen A with force of 400 N

The measured maximum displacements for the milled specimen and the sandblasted specimen differ by merely ca 1.5  $\mu\text{m}$ . As opposed to the previously discussed measurements, the ones shown in Fig. 11 were not preceded by a preliminary cycle of loading to 100 N. The LED and PD indicators and the LED characteristics shown in Fig. 7 facilitate estimations in such measurements. They were used to estimate all the displacement components in the contact under load (Table 3) to determine the degree of agreement with the real measurements.

Table 3. Estimates of deformation components of specimen loaded with force of 400N in first cycle

FORECAST for 400N: (Unloading from: 400N)	Specimen made of Al alloy			
	A/AL./SB		A/AL./M	
Deformation	$\mu\text{m}$	%	$\mu\text{m}$	%
- nonlinear NED:	4.4	25	4.3	26
- plastic PD:	7	40	6	36
- linearly elastic LED:	6.2	35	6.15	38
Deformation M = NED+PD+LED	17.6	100	16.4	100
M - measured for 400N (from roughness profiles):	16.5	100	15.0	100

In the forecast shown in Table 3 the difference between the maximum deformations for the milled specimen was estimated to amount to 1.2  $\mu\text{m}$  while in the measurement (Fig. 11) this difference amounted to 1.5  $\mu\text{m}$ . In a similar way, using the indicators shown in Fig. 7 one can predict real contact deformation for any loads below 400 N.

## 8. CONCLUSION

On the basis of the experimental results it was decided to use specimens of type A in further research since they are much easier and cheaper to make and complicate less the measurement process in comparison with monolithic specimens type B. It has been shown that the effect of the additional contact in specimens A on measurement results is negligible. This means that the fixing force ensured by the negative pressure system is sufficient to prevent uncontrolled displacements.

In the case of the aluminium specimens, the kind of machining (surface roughness) has a relatively small effect on contact deformations – only the plastic deformations in the contact change, amounting to about 35–37%. In the case of the steel specimens, this is three times less. Whereas the share of nonlinear elastic deformations in the aluminium specimens is almost twice smaller than in the steel specimens under load.

The determined NED characteristics and the LED and PD indicators can be used not only to predict the behaviour of tested contact pairs after the first loading and the subsequent loadings, but also to verify the FE contact deformation models developed by the author. The models should make it possible to determine first of all the contact deformations which occur during the first loading since such cases are very common during the machining of workpieces held in fixtures or jigs.

## ACKNOWLEDGEMENTS

*The investigation have been carried out as part of the project WIPO **INNOTECH-K1/IN1/75/155671/NCBR/13** funded by the Polish National Center for Research and Development (NCBiR). The measurements by means of the TalySurf CCILite (Taylor Hobson) profilometer were carried out in the Laboratory of Mechatronics and Machine Vision, Institute of Production Engineering and Automation, Wrocław University of Technology. Calculations have been carried out in Wrocław Centre for Networking and Supercomputing (<http://www.wcss.pl>), grant No.109.*



Wrocław University of Technology



Narodowe Centrum  
Badań i Rozwoju

## REFERENCES

- [1] MACIOŁKA P., JEDRZEJEWSKI J., GROCHOWSKI M., 2014, *A device for the experimental investigation of surface contact under load*, Journal of Machine Engineering, 14/3, 97–112.
- [2] MATHIA T., PAWLUS P., WIECZOROWSKI M., 2011, *Recent trends in surface metrology*, Wear, 271/3-4, 494–508.
- [3] GRYBOŚ R., 1971, *The maximum impact force-restitution coefficient dependence*, Mechanika Teoretyczna i Stosowana, 2/9, 263–283, (in Polish).
- [4] TABOR D., 1951, *The Hardness of Materials*, Clarendon Press, Oxford.
- [5] KOSTEK R., 2012, *The modelling of loading, unloading and reloading of the elastic-plastic contact of rough surfaces*, Journal of Theoretical and Applied Mechanics, 50/2, 509–530.
- [6] VU-QUOC L., ZHANG X., LESBURG L., 2000, *A normal force-displacement model for contacting spheres accounting for plastic deformation: force-driven formulation*, Journal of Applied Mechanics, ASME, June 2000, 67, 363–371.

- 
- [7] NIEMCZEWSKA-WÓJCIK M., SŁADEK J., TABAKA M., WÓJCIK A., 2014, *Product quality assessment – measurement and analysis of the surface topography*, Metrology and Measurement Systems, Vol. XXI/2, 271-280.
- [8] NIEMCZEWSKA-WÓJCIK M., MAŃKOWSKA-SNOPCZYŃSKA A., PIEKOSZEWSKI W., 2013, *The investigation of wear tracks with the use of noncontact measurement methods*, Archives of Civil and Mechanical Engineering, 13/2, 158-167.